# RESISTANCE PREDICTION USING ARTIFICIAL NEURAL NETWORKS FOR PRELIMINARY TRI-SWACH DESIGN

**Lt(N) A Carter**, Royal Canadian Navy, Canada, **E Muk-Pavic**, University College London and **T McDonald**, Atkins Oil & Gas, UK

**SUMMARY**

Due to the novel hull form design, at present no standard series or full-scale data is publicly available to predict Tri-SWACH resistance during the preliminary ship design process. This work investigates the viability of using an Artificial Neural Network (ANN) to quickly predict total resistance for preliminary Tri-SWACH design.

An ANN was trained using total resistance experimental data obtained from model tests, which varied side hull arrangements. The results highlight strong correlation for model resistance prediction. A Tri-SWACH case study was then developed which had side hull geometric properties different to any previously used to train the ANN. The results, validated against CFD predictions, mimicked the resistance pattern generated by other model experimental data, providing confidence in the ANN's ability to function as a resistance prediction tool.

This work demonstrates the viability of ANN to assess Tri-SWACH resistance as part of a preliminary design process. These results suggest that ANNs can be effective tools for assessing performance given relevant training data.

**NOMENCLATURE**

| | |
|---|---|
| $C_{AA}$ | Air or wind resistance coefficient |
| $C_{AP}$ | Appendage resistance coefficient |
| ANN | Artificial neural network |
| $C_F$ | Frictional resistance coefficient of a body |
| $C_{F0}$ | Frictional resistance coefficient of a corresponding plate |
| Fr | Froude number |
| $C_A$ | Incremental resistance coefficient for model ship correlation |
| ν | Kinematic viscosity ($Nm/s^2$) |
| $X_{CB}$ | Longitudinal centre of buoyancy (m) |
| MAE | Mean absolute error |
| MSE | Mean square error |
| b | Neuron bias |
| p | Neuron input parameter |
| a | Neuron output parameter |
| w | Neuron weight |
| $C_R$ | Residuary resistance coefficient |
| ΔC | Resistance interference effects coefficient |
| Re | Reynolds number |
| RMSE | Root mean squared error |
| $R_{TM}$ | Total model resistance (N) |
| $C_T$ | Total resistance coefficient |
| Tri-SWACH | Trimaran-Small Waterplane Area Centre Hull |
| $C_V$ | Viscous resistance coefficient |
| $C_W$ | Wave-making resistance coefficient |

## 1. INTRODUCTION

### 1.1 BACKGROUND

Hull resistance calculations for Trimaran-Small Waterplane Area Centre Hull (Tri-SWACH) hull forms require a novel approach due to a lack of full-scale ship data and standard series data sets. Artificial Neural Networks (ANNs) have been previously used in a wide variety of naval architectural applications generating very positive results [1]. However, the complex wave interactions and interference effects exhibited by multi-hulled vessels pose a challenge for all prediction methods.

Previous work has been conducted into ANNs' applicability as prediction tools for multi-hull resistance. Of specific interest to this project, ANNs were developed and shown to provide a successful alternative to more traditional statistical regression models for both catamaran [2] and trimaran [3] hull forms. These two reports provide fidelity in the ANN's ability to successfully map the complex resistance patterns associated with multi-hulled vessels.

### 1.2 Tri-SWACH HULLFORMS

The Tri-SWACH combines the concepts of a trimaran and Small Waterplane Area Twin Hull (SWATH) hull forms. Tri-SWACH hull forms have slender side hulls outboard a single small waterplane centre hull. The side hulls provide stability while the centre hull has a minimal water plane area to reduce wave excitation and hence motions. Compared to a similar displacement monohull the Tri-SWACH hull form has increased wetted area (and hence frictional resistance) however the very slender waterplane significantly reduces residuary resistance. The Tri-SWACH allows the designer to maximise deck space and enhance seakeeping performance while minimizing any negative resistive effects. Figure 1 highlights the main features of a Tri-SWACH hull form.

While few examples have been built, significant interest in the Tri-SWACH hull form currently exists for specific niche roles. The hull form has been identified as a promising alternative for the offshore wind turbine industry due to the potential seakeeping benefits. Offshore wind farm efficiencies are decreased by turbine

 

downtime due to failure or maintenance. Therefore the importance of the accessibility for personnel is significant. Ship-to-turbine personnel transfer operations pose significant risk to maintenance staff; reductions to relative motions between the turbine platform and the support vessel are highly desirable. However this must be balanced against vessel deployment speed and range. Austal has developed a line of offshore wind turbine support vessels, the Wind Express Tri-SWATH series [4], and the Norwegian shipbuilder Fjellstrand has developed a similar concept, the Wind Server series, which again are wind farm support vessels [5].

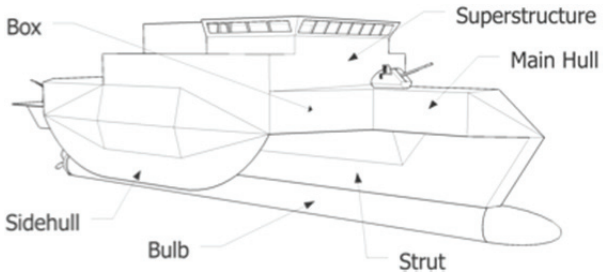


Figure 1 Example of a Tri-SWACH hull with common nomenclature

(a) Austal Wind Express Series Tri-SWATH [4]

(b) Fjellstrand's Wind Server Series Tri-SWACH [5]

Figure 2 Tri-SWACH Based Offshore wind turbine/farm support vessel

The advantages afforded by the Tri-SWACH design may also represent an alternative for some naval and commercial applications. Reduced motions and resistance could benefit the ferry and cruise industry by offering more comfortable journeys and reduced fuel costs. The gains in upper deck space, reduced resistance and increased seakeeping performance could improve profit margins for commercial companies by cutting fuel costs while expanding payload size. Military applications would gain from the increased upper deck space and enhanced seakeeping performance by broadening the operational envelopes for small boat, helicopter and unmanned aerial vehicle (UAV) operations.

### 1.3 ACCESS PROGRAMME EXPERIMENTAL DATA

The Atlantic Centre for the Innovative Design and Control of Small Ships (ACCeSS) has an ongoing research programme exploring Tri-SWACH performance and design. ACCeSS was founded in 2002 and is focused on establishing an environment where engineering disciplines associated with hull design and ship automation can be brought together within the context of the total ship system architecture. A recent joint programme (involving University College London (UCL), the Stevens Institute of Technology (SIT), the Webb Institute, and the United States Naval Academy (USNA)) has conducted a series of Tri-SWACH model tests to investigate Tri-SWACH resistance and the effect of various side hull configurations. This built on work previously conducted at Webb Institute [6] on the resistance effects of side hull locations for trimaran hull forms.

The Tri-SWACH hull resistance experimental data was obtained through various model towing tank tests conducted across the ACCeSS consortium. The experimental data was obtained by testing a single model built at Webb Institute, shown in Figure 3. The model's key characteristics are listed in Table 1.

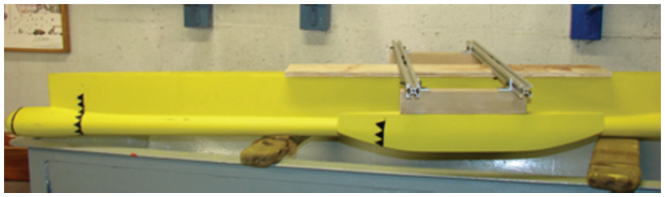

Figure 3 Towing tank Tri-SWACH model used to collect experimental model resistance data [7]

Table 1 Tri-SWACH model characteristics [7]

| | **Centre Hull** | **Side Hull** |
|---|---|---|
| Length | 2.134 m | 0.613 m |
| Beam (Waterline) | 0.064 m | 0.031 m |
| Draught | 0.171 m | 0.057 m |
| Displacement | 0.391 $m^3$ | 0.012 $m^3$ |
| Wetted Surface Area | 0.577 $m^2$ | 0.058 $m^2$ |
| LCB | 1.014 m | 0.306 m |

The experimental series investigated changes to side hull locations and orientation. All three institutions used an identical experimental method to conduct tank tests on the Tri-SWACH model [8]. Table 2 indicates the side hull configurations tested and Figure 4 shows the side hull location relative to the forward perpendicular

and centreline of the central hull. These configurations are denoted by the sidehull's longitudinal and lateral locations, e.g. "fwd-outboard". The USNA also performed tests using three different side hull splay angles (canted the side hulls outwards at angles of 0°, 0.5° and 1.5° from the centreline). The experiments resulted in a data set of 507 distinct configurations and speeds that could be employed for ANN training, validation, and testing.

Figure 5 illustrates experimental results for the mid inboard Tri-SWACH configuration as indicated in Figure 4. The data points indicate experimental results obtained from model tests at USNA, SIT and Webb. The lines indicate CFD results for an identical geometry obtained from two numerical resistance prediction codes: Michlet [9], which employs thin ship theory; and AEGIR [10], a higher order potential flow theory code. The results show distinctive humps arising from the interaction of the main

Table 2 Test matrix for ACCeSS programme towing tank tests [8]

| **Lateral Position** | **Inboard** | | | **Mid** | | | **Outboard** | | |
|---|---|---|---|---|---|---|---|---|---|
| **Longitudinal Position** | **Fwd** | **Mid** | **Aft** | **Fwd** | **Mid** | **Aft** | **Fwd** | **Mid** | **Aft** |
| Webb Institute | x | x | x | x | x | x | x | x | x |
| SIT | | x | | x | | x | | x | |
| USNA | | x | | | | x | | | |

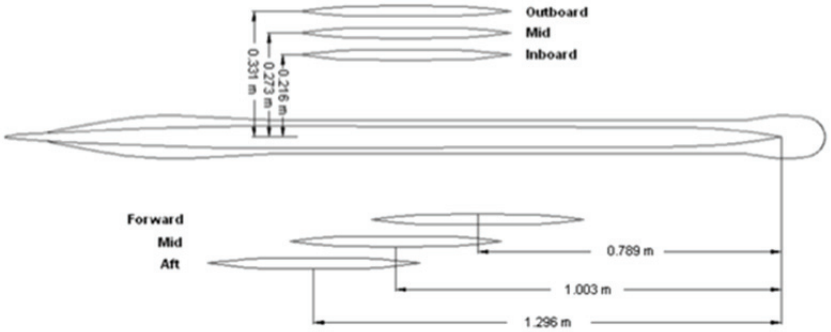


Figure 4 Tri-SWACH model side hull locations for towing tank tests

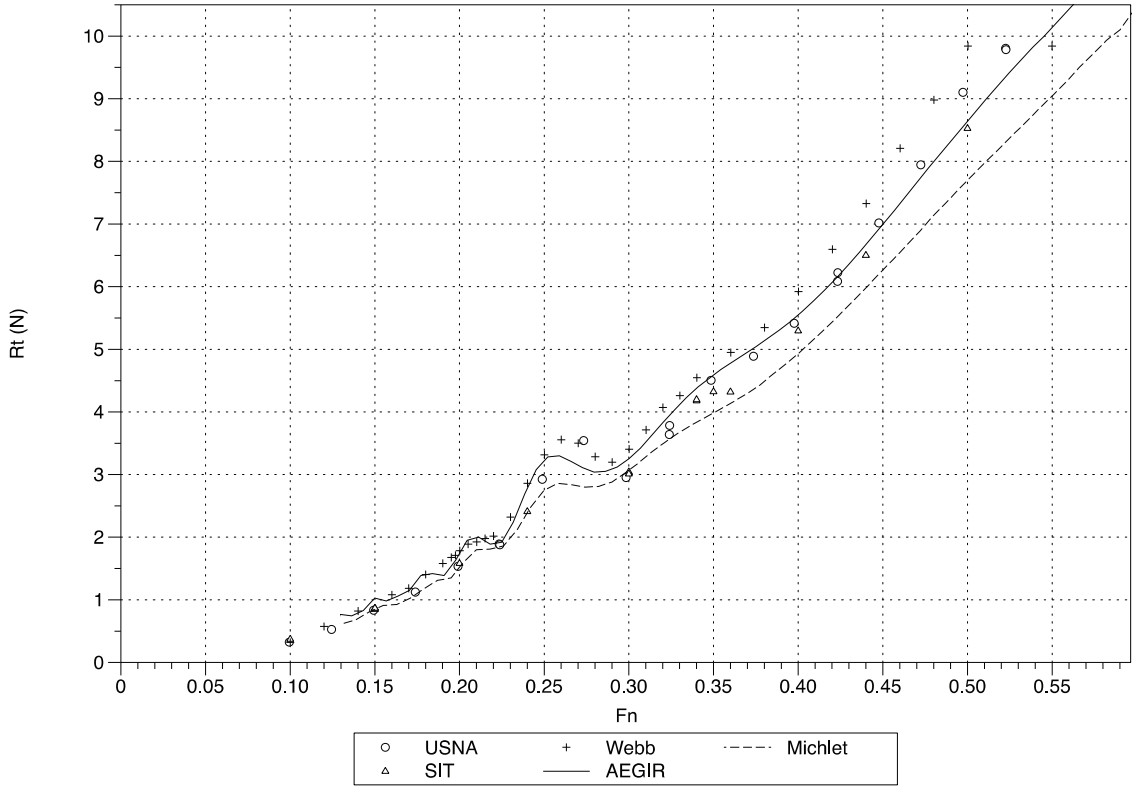


Figure 5 Comparison of experimental data to computational fluid dynamics simulation performed by the ACCeSS consortium [8]

hull and side hull wave systems at different vessel speeds. These were present in all tested model configurations, however the magnitude and speed at which they occurred differed as the side hull arrangement was changed. With regard to the CFD code results, AEGIR predictions are close to experimental data while the Michlet values demonstrate a slight under prediction; in particular, the numerical codes seem to under-predict performance in the "hump region" (corresponding to Froude numbers of 0.25-0.30) and also appear to incorrectly identify the Froude number corresponding to the hump. Again, similar observations were made for all tested model configurations.

## 1.4 ARTIFICIAL NEURAL NETWORKS

ANN technology provides an appealing alternative to traditional modelling techniques for complex, non-linear relationships. They are in essence a sophisticated mapping tool that develops a relationship between input parameters and target output values. Figure 6 shows two indicative neural networks.

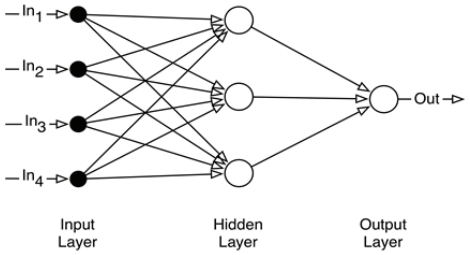


(a) One layer network

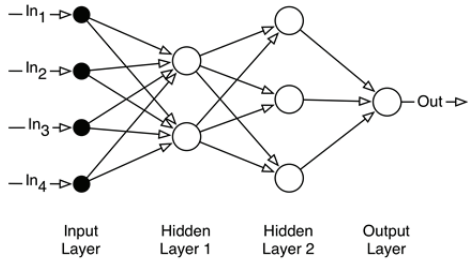


(b) Two layer network

Figure 6 Examples of basic neural network topology [11]

Neurons are connected together in several layers, interconnected by inputs and outputs. The output of the overall ANN is computed from the collective outputs of each individual neuron on the many layers. Therefore, the power of an ANN comes from its collective behaviour as a network of interconnected neurons.

An individual neuron's output is a function of the sum of the neuron's inputs, $p_{1,2,3...R}$ , multiplied by weighting, $w_{1,2,3...R}$, plus a bias value, $b$. A transfer function, $f$, converts this into the neuron's output, $a$ [12]. The basic mathematical relationship established within a neuron is of the form as illustrated in Figure 7:

$$a = f(w_1p_1 + w_2p_2 + w_3p_3 + \cdots + w_Rp_R + b)$$

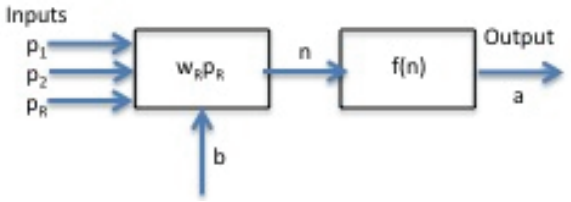


Figure 7 Schematic diagram of an artificial neuron [12]

The transfer function, or activation function, controls the amplitude of a neuron's output. Typically, the output is either between the range of 0 to 1 or -1 to 1. Commonly used activation functions are shown in Figure 8.

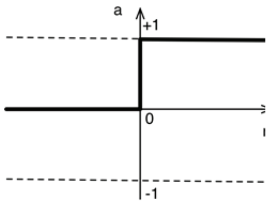


(a) Hard-Limit transfer function

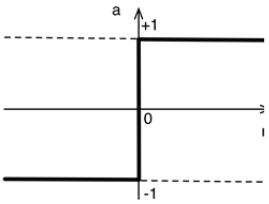


(b) Symmetric hard-limit transfer function

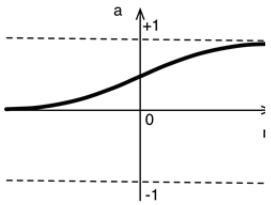


(c) Tan-Sigmoid transfer function

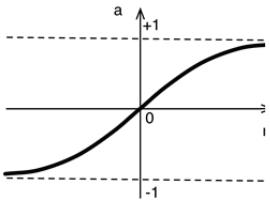


(d) Log-Sigmoid transfer function

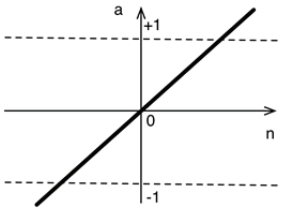


(e) Linear transfer function

Figure 8 Common activation functions used in neural networks [15]

The number of hidden layers and number of neurons per layer are governed by the complexity of the non-linear relationship that is being modelled; the more complex the relationship, typically, the more layers and more neurons required. However, it is prudent to avoid over-complex ANNs because they have a tendency to "overfit" the data, i.e. rather than acquire the relationship between input and target values, the ANN "memorizes" the data, and its performance rapidly decreases when introduced to new test data. The activation function has little effect on the performance of the ANN [12].

### 1.5 LEARNING AND GENERALIZATION

Arguably, the most remarkable attribute of an ANN is its ability to learn. Similar to the metabolic change in biological synapses within the brain, a learning process is applied to the neurons within an ANN, allowing it to adapt and "learn" through interaction with its environment or exposure to an information source. "Learning in a neural network is normally accomplished through an adaptive procedure, known as a learning rule or algorithm, whereby the weights of the network are incrementally adjusted so as to improve a predefined performance measure over time" [13].

Through a process of computation and feedback, the individual weights are adjusted to reduce the error in each training pair; where each iteration is defined as an epoch. As the ANN moves through each epoch, weights should begin to converge to a set of values, which adequately maps the inputs to the output. For all training patterns, when the errors have been reduced to an acceptable level, "learning" has been achieved [14]. Essentially, the ANN develops an algorithm to map the inputs to an output by adjusting its weights through the process of error reduction.

In this work the Levensberg-Marquardt method has been adopted as a training algorithm. While numerous other training algorithms are possible, the Levensberg-Marquardt method is commonly employed due to its rapid convergence. It has been reported to perform well on function-fitting problems with a low number of weights (but requires large amounts of memory and computation time), so is well suited to this study [15].

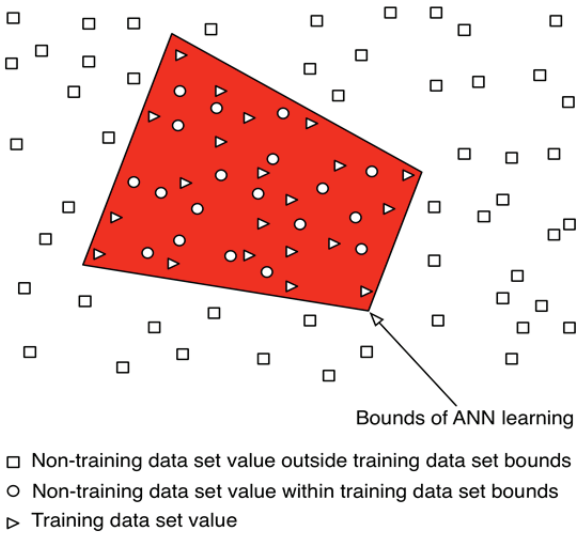


Figure 9 Concept of generalization bounds for ANN learning [14]

ANNs work on the basis of generalization, which is defined as the "act or process whereby a learned response is made to a stimulus similar to but not identical with the conditioned stimulus" [16]. So, although trained using known data points, neural networks are capable of accurately interpolating to predict values bounded by the training data. This is achieved by the neural networks ability to learn. Rather than making broad generalizations, the more data the ANN is trained on, the better it understands the relationship between the input and target values. Outside of the bounded area, the neural network has little understanding of the input-target relationship, and hence its ability to predict values decreases markedly [14], as shown in Figure 9.

### 1.6 FEED FORWARD NETWORKS

Throughout this work, the basic feed forward ANNs are used because of their excellent mapping characteristics; they are the most common form of ANNs due to the wide range of applications afforded by their architecture. Feed forward networks are designated as such because the signal is only permitted to pass from an input node to an output node in the forward direction; signals do not propagate in the lateral or backward direction between neurons in a network.

## 2. Tri-SWACH RESISTANCE

Due to the novel design, the resistance effects of a Tri-SWACH hull form are relatively unknown. Although Austal and Fjellstrand have undoubtedly conducted their own research into Tri-SWACH resistance for their respective designs, this information is not publicly available. Furthermore, no standard series data have been developed for Tri-SWACH hull forms.

The International Towing Tank Conference Performance Committee provided general recommendations on how to examine the total resistance of multi-hull vessels [17]. Their recommendations highlight that traditional frictional component decomposition approaches are applicable for multi-hulls if interaction effects are accounted for. Allowing a total resistance coefficient $C_T$ to be developed from frictional $C_{F0}$, residual $C_R$ and wave $C_W$ components plus an additional coefficient $\Delta C$ containing other resistance elements (e.g. ship-model correlation, aerodynamic and appendage resistance), hence:

$$C_T = C_{F0} + C_R + C_W + \Delta C$$

Other authors assert that simple theoretical models (i.e. thin ship theory) cannot solely be used to accurately predict total ship resistance for multi-hull vessels due to the complexity of the flow patterns around the hulls [18]. Model testing remains one of the more effective methods of accurately determining the total resistance of multi-hulled ships. These tests can allow the quantification of both vessel total resistance and interaction effect between the hull forms; although scaling can introduce uncertainties.

 

Both approaches take considerable time and effort to develop suitable results. This study explores applying an ANN to rapidly determine total resistance from a limited range of inputs.

### 2.1 PRINCIPAL PARAMETERS AFFECTING Tri-SWACH RESISTANCE

Investigation of multi-hulled vessel resistance patterns emphasised the significant effect the central hull had on the resistance of the outriggers (depending upon their lengthwise position). Conversely, it was noted that the outriggers are less influential on the wave-making resistance of the central hull, although a dependency on outrigger lengthwise position was observed [18]. This suggests that, like trimarans, the configuration of the side hulls plays a role in the total resistance characteristics of the Tri-SWACH. Additionally, it was noted, "the interference effects between hulls directly influences the wave-making resistance. High length-to-beam ratios and beam-to-draught ratios greatly reduce the disturbances generated by the hulls" [18]. Table 3 lists the important parameters that have a direct influence on resistance behaviour of a Tri-SWACH.

Table 3 Principal Proponents of Tri-SWACH Resistance

| ***Parameters*** | ***Symbol*** |
|---|---|
| Length centre hull | $L_{CH}$ |
| Length side hulls | $L_{SH}$ |
| Beam overall | $B_{OA}$ |
| Strut thickness | $Th_{Strut}$ |
| Longitudinal centre of buoyancy | $X_{CB}$ |
| Centre hull wetted surface area | $S_{CH}$ |
| Side hull wetted surface area | $S_{SH}$ |
| Total displacement | $\nabla_{Tot}$ |
| Centre hull trim | $t_{CH}$ |
| Side hull trim | $t_{SH}$ |
| Froude number | Fr |
| Length-to-beam ratio of centre hull | $\lambda_{CH}$ |
| Length-to-beam ratio of side hulls | $\lambda_{SH}$ |
| Length-to-beam ratio of overall Tri-SWACH | $\lambda_{Tot}$ |
| Side hull slenderness ratio | $L_p/D_p$ |
| Ratio of the transverse spacing of the side hulls relative the central hull | %Trans |
| Ratio of the longitudinal spacing of the side hulls relative the central hull | %Long |
| Side hull angles of attack | $\alpha_{SH}$ |
| Side hull splay angle | SA |

## 3. METHOD

The following method was adopted to develop the ANN:

- Experimental data was collected and the principal parameters which directly influence total Tri-SWACH resistance were identified;
- The experimental data was divided into a Training Data Set and a Test Data Set, where the Test Data Set was randomly selected and represents 10% of available data;
- The experimental data was processed to improve the training speed of ANN;
- The number of weights, hidden layers, and activation functions were selected;
- The ANN was trained using the Training Data Set;
- Once trained, the ANN performance was tested using the Test Data Set; and
- The Test Data Set outputs were analysed using Mean Absolute Error (MAE) and Mean Absolute Percentage Error (MAPE), as defined in Annex A, to verify the ANN performance.

The best performing ANN (lowest MAE) was selected. The developed ANN was validated using a case study model and compared against Michlet CFD code results. This permitted the ANN's ability to interpolate results to be examined, and hence validate its capacity to function as a resistance prediction tool.

### 3.1 KEY PARAMETERS SELECTION

Earlier, the principal parameters that influence Tri-SWACH resistance were identified and listed in Table 3. However, an important aspect to note is that ANN training is not improved by using parameters, which remain constant over their entire range. Constant parameters provide little aid to the neural network during training in identifying the underlying relationship between input and target values. As a result, they are accounted for by an adjustment of the bias in the final network layer. Therefore, all constant value input parameters, based on the physical dimensions of the Tri-SWACH model, were ignored since the same model was used to collect all experimental data; the exception being the side hull positions and splay angles. Removing the constant rows significantly reduced the number of input parameters available to train the ANN. This could significantly affect the ANN's ability to acquire the intrinsic relationship between the input parameters and the target values. With constant value parameters removed, the parameters listed in Table 4 were used to predict Tri-SWACH total model resistance.

Table 4 Key parameters in dimensional form that affect Tri-SWACH hull resistance

| ***Parameter*** | ***Units*** |
|---|---|
| Froude Number | - |
| Transverse Separation of Side Hulls Relative to Centre Hull | m |
| Longitudinal Separation of Side Hulls Relative to Centre Hull | m |
| Splay Angle of Side Hulls | ° |
| Trim | m |

### 3.2 ANN TRAINING STUDY

During this study, six different ANNs were trained to explore their performance at acquiring the relationship between the input parameters and the target values. All had a single hidden layer but the number of neurons in

the hidden layer ranged from one to six. The constraint of six ANN configurations was imposed by the general guidance that the number of weights in the ANN must be ten times less than the number of data vectors in the training data set, see Table 5.

Table 5 ANN configuration limits from training data set

| $N_{weights} = 10 \times \left(N_{input\ parameters} \times N_{neuron\ weights}\right) + N_{bias\ values}$ | |
|---|---|
| 6-neurons | $10 \times (5 \times 6 + 6 = 36) < 375$ |
| 7-neurons | $10 \times (5 \times 7 + 7 = 42) > 375$ |

Note, of the original 507 experimental data points, 375 remained in the training data set once the test data set values were removed. This general direction guarantees that overfitting and data memorization does not occur, thus ensuring the validity of the results. In this case, ANN configurations that exceed six neurons increased the likelihood of overfitting and data memorization and were avoided.

For the six different ANNs examined, the one-neuron ANN configuration employed a *pure linear* activation function. This ANN configuration linearly maps the inputs to the target values and allows the weights and bias values to be examined. The other ANN configurations employed a hyperbolic tangent (*tansig*) activation function:

$$tansig(n) = \frac{2}{1 + e^{-2n}} - 1 \qquad \text{Eq. 1}$$

This function (shown in Figure 8c), is mathematically equivalent to *tanh*, but can be processed faster increasing neural network's speed [13].

### 3.3 ANN PERFORMANCE VALIDATION

The performance of each ANN can be quantified by a variety of statistical methods (as detailed in Annex A). In the case of this investigation, the MAE and MAPE were used as they provide a more tangible measure of error by giving the average deviation from the actual target value. The ANN configuration with the lowest MAE/MAPE value represents the best configuration.

## 4. RESULTS

Table 6 shows the MAE/MAPE results for each trained ANN configuration tested. The trained ANN with six neurons in the hidden layer had the highest accuracy of 9.19% MAPE. Figure 10 illustrates the correlation between the predicted total model resistance results generated by the six-neuron, single hidden layer trained ANN and the actual experimental data for total model resistance selected from the independent test data set. Note that the experimental data is randomly selected and does not represent the resistance for one configuration.

Table 6 Test Data Set MAE/MAPE Results for Each ANN Configuration

| ***Number of Hidden Layer Neurons*** | ***MAE*** | ***MAPE*** |
|---|---|---|
| One | 0.4262 | 33.96% |
| Two | 0.3165 | 13.49% |
| Three | 0.3108 | 10.64% |
| Four | 0.3052 | 10.32% |
| Five | 0.3365 | 11.99% |
| Six | 0.2833 | 9.19% |

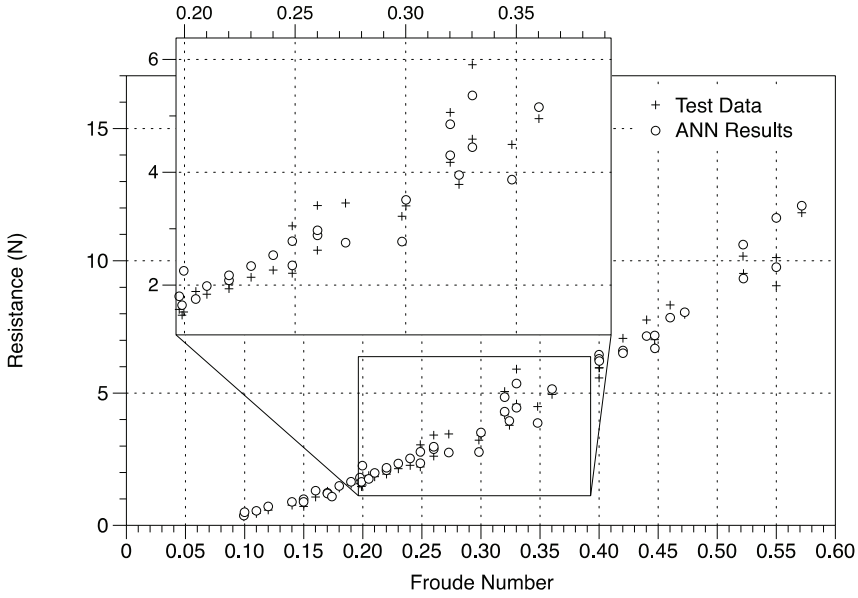


Figure 10 Correlation between total model resistance from experimental data and ANN results

Analysing Figure 10, it can be ascertained that the trained ANN has good prediction abilities for total model resistance values associated with low Froude numbers. This is likely to be a result of a significant number of training data points in this region which permitted the ANN to develop a good understanding of the relationship between the input parameters and the target values. The accuracy of the trained ANN appears to decrease, although not significantly, as the Froude number increases. The one area of concern is the apparent reduction of accuracy in the Froude range of 0.25 to 0.40. Critically, based on the experimental results, this is an area of significant interest during the preliminary ship design as it coincides with the typical location of the resistance humps and potential cruise speed. Nevertheless, even in the Froude range of 0.25 to 0.40 the predictions are reasonable. In fact, for the preliminary design stage, the results would likely be sufficient to generate satisfactory resistance predictions to allow the design to mature without drastic alterations at a later stage.

The probable source for the lack of predictability in this region is the large variation incurred in this Froude number range in the experimental data. This could prohibit the ANN from appropriately developing the input-target relationship during training. The large variation is due to the high dependency on Tri-SWACH hull configuration within this region. Both transverse and longitudinal spacing of the side hulls relative to the centre hull affect the prismatic and main resistance humps [16]. As such, due to the experimental method employed whereby each institution tested different Tri-SWACH configurations, there is little repetition of configuration trials, and therefore, less training data points available within this region to accurately train the ANN. With little training data to fully expose the input-target relationship in this Froude number range, the accuracy of the ANN prediction capabilities is impaired.

As shown in Figure 5, the scatter in the ACCeSS consortium experimental data was minimal. However, even minimal scatter can influence the accuracy of the ANN generated results since an ANN's accuracy is highly dependent on the accuracy of the data used to train it; any scatter will be amplified by the ANN due to the inherent inaccuracies involved in the learning process. Increasing the volume of training data can reduce the error propagation. In this case, the scatter in experimental data at higher Froude numbers could be a contributing factor in the increased variations between the ANN generated results and the experimental values at Froude numbers above 0.30.

## 5. CASE STUDY

A case study was developed to provide an indication of the ANN's performance as a potential resistance prediction tool by confirming the ANN's ability to interpolate and predict Tri-SWACH resistance based on numbers not previously trained or tested on. The case study model is a hypothetical Tri-SWACH model whose hull geometry is identical to that of the ACCeSS programme, however, the side hull positions are different from any tested in the ACCeSS programme's experimental towing tank tests. The longitudinal spacing of the side hulls is 1.10 m from the stem of the centrehull, which lies between the mid and aft locations of the ACCeSS experiments, and the transverse spacing is 0.250 m, which lies between the mid and inboard ACCeSS programme test configurations.

Table 7 and Figure 11 display the physical parameters of the case study Tri-SWACH model.

Table 7 Case study Tri-SWACH model parameters

| *Parameter* | *Model* |
|---|---|
| Transverse Side Hull Clearance | 0.250 m |
| Longitudinal Side Hull Clearance | 1.100 m |
| Side Hull Splay Angle | 0° |
| Maximum Speed | 5.3 kts |
| Maximum Speed | 2.714 m/s |
| Maximum Fr | 0.593 |
| Maximum $Re_{CH}$ | 6.86E+06 |
| Maximum $Re_{SH}$ | 1.97E+06 |

Using the trained ANN the case study values were simulated. The results displayed in Figure 12 were obtained over a Froude number of 0.1 to 0.6.

To confirm the accuracy of the ANN generated results for the case study Tri-SWACH, four Webb Institute experimental results, which had similar configurations to the case study Tri-SWACH, were plotted. The side hull arrangements of the four comparison models are listed in Table 8.

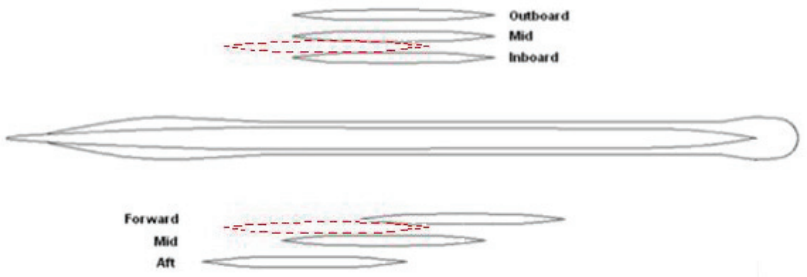


Figure 11 Overlay of case study side hull arrangement compared to ACCeSS programme's tested side hull locations

Table 8 Side hull arrangement characteristics of similar Tri-SWACH configurations tested experimentally at Webb

| | ***Case Study Model*** | ***Mid-Mid Configuration*** | ***Mid-Inner Configuration*** | ***Aft-Mid Configuration*** | ***Aft-Inner Configuration*** |
|---|---|---|---|---|---|
| Longitudinal Spacing (m) | 1.100 | 1.003 | 1.003 | 1.290 | 1.290 |
| Transverse Spacing (m) | 0.250 | 0.273 | 0.216 | 0.273 | 0.216 |
| Splay Angle (°) | 0 | 0 | 0 | 0 | 0 |

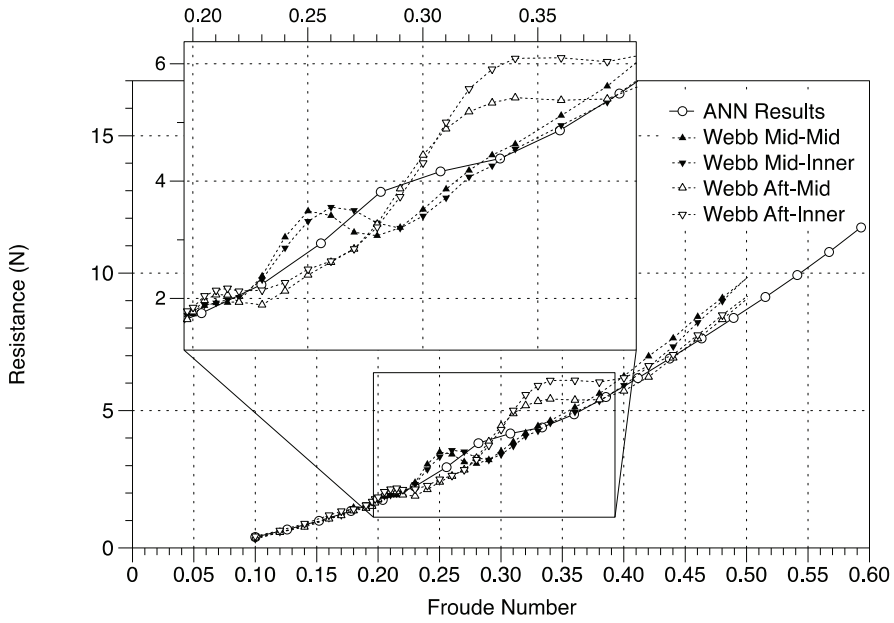


Figure 12 Comparison of case study ANN predicted resistance to similar Tri-SWACH configurations tested experimentally

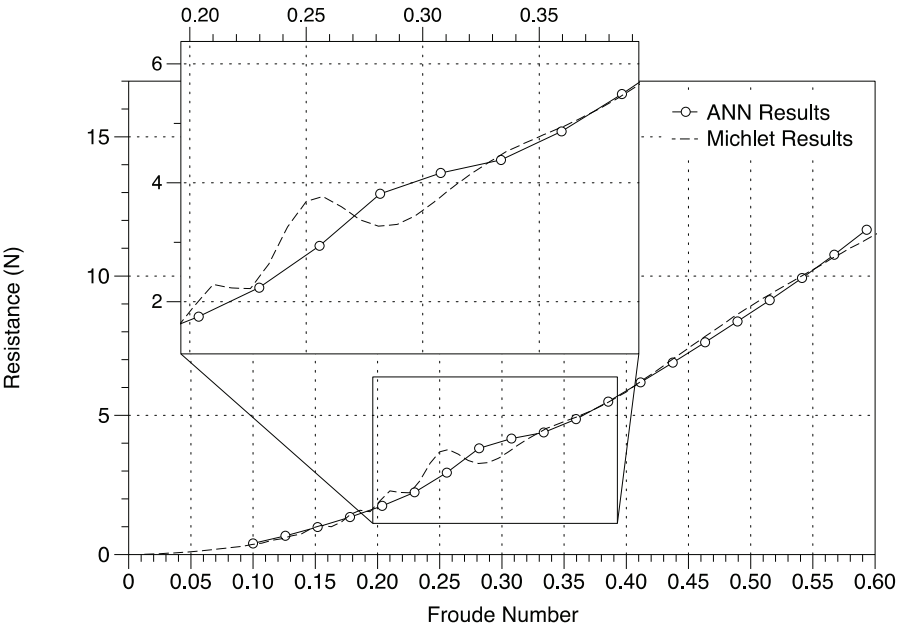


Figure 13 ANN results compared to numerical prediction

Comparison to the numerical resistance prediction results obtained for the specific case study configuration reinforces the ANN's ability to function as a resistance prediction tool. Figure 13 compares the ANN output to data obtained from a numerical thin ship theory based code – Michlet. Michlet was selected, as it typifies the rapid analysis tools often employed within concept design. While not able to match the accuracy of a higher order CFD code such as AEGIR, Michlet captures key resistance characteristics, e.g. the locations of resistance "humps". While the ANN and numerically predicted resistance humps do not line up, drawing on the observations from Figure 5, it was evident that Michlet tends to shift the main and prismatic humps to the left

(i.e. lower Froude numbers). Therefore, for the assessed configuration the main hump would actually lie slightly to the right (at a higher Froude number) closer to the ANN generated resistance prediction.

The shape of the main hump could likely be improved by increasing the case study data points; however, as a tool for preliminary ship design, the fact that the ANN is capable of determining the Froude range of the main hump would be adequate enough to allow the design process to progress. Later in the design process a more accurate prediction of Tri-SWACH resistance would need to be determined but by that point model testing would be a viable option.

The case study results provide fidelity in the ability of the ANN to perform as a Tri-SWACH resistance prediction tool for this particular Tri-SWACH model. The authors remain confident that with further work, this confidence in the ANN's potential to predict resistance values will strengthen and clearly demonstrate the ANN's ability to be a resistance prediction for Tri-SWACH preliminary ship design. The results yielded in this investigation are encouraging and demonstrate the ANN's capacity to model complex relationships associated, in particular, to multi-hull design but further support continued efforts to utilize ANNs in marine applications.

## 6. CONCLUSIONS

The results confirm the ANN's ability to perform as a resistance tool for Tri-SWACH preliminary design for this particular model. Research and experimental data has shown that the prismatic and main resistance hump for Tri-SWACH vessels is dependent on the physical configuration of the side hulls relative to the centre hull. Careful consideration of Tri-SWACH configuration can lead to reduced resistance characteristics potentially permitting better performance and reduced fuel consumption, especially at high speeds. Research has also confirmed that Tri-SWACH resistance is dependent on a large number of parameters, indicating a high level of complexity, which would require sophisticated models to accurately understand and interpret its behaviour.

The ANN is capable of producing a resistance prediction despite the complex nature of Tri-SWACH resistance. Although not accurate enough for a final design, the results generated by the ANN would be sufficiently accurate for preliminary ship design, permitting the design process to progress based on approximate resistance values. The current ANN has a mean average percentage error of approximately 10%; and with additional experimental data available, it is believed that this error could be greatly reduced.

The results also further support previous work, which highlighted the success application of ANNs to predict performance characteristics of other multi-hull vessels; specifically the work carried out by Dr. Rick Royce at Webb Institute on trimaran hull forms [3]. Given the success obtained in using ANNs for resistance prediction of these two multi-hull vessel types, the authors are confident that ANNs could be trained and used with a wide assortment of hull form types, as a means of predicting resistance performance. The ability to use ANNs to simplify the prediction methods to obtain multi-hull resistance could be of interest to military and offshore conceptual design teams where, increasingly, multi-hulled vessels are proving to be attractive options due to their superior seakeeping performance and large upper deck area.

Overall, the results presented in this paper demonstrate the ANN's potential to be a resistance prediction tool for Tri-SWACH preliminary ship design. It should be noted that total ship resistance can be determined using a scaling method of the user's preference.

### 6.1 FUTURE WORK

The results presented in this paper are an encouraging demonstration that an ANN can be used to develop an effective Tri-SWACH resistance prediction tool; however, several areas exist where further developments are possible.

In conversation with ACCeSS partners, it has been recommended that the model be tested using the side hull configuration identified in the case study to verify the accuracy of the ANN generated results. Although a comparison was made to a numerical thin ship theory based code, the inherent limitations and assumptions within the code prevent an accurate assessment of the true performance of the trained ANN as a resistance prediction tool. Direct comparison to experimental data would provide a true evaluation of the ANN's performance.

Further areas to investigate include increasing the range of experimental data through further testing of different model sizes with different geometric properties. The current trained ANN is limited to predicting resistance values within the bounds of the extreme side hull configurations of the tested model. Additional model tests would also allow the ANN to expand the applicability envelope to a range of numerous hull parameters, as listed in Table 3.

The recommendation would be to first conduct towing tank tests using extreme side hull configurations of the current model, which represent realistic extremes of this Tri-SWACH design. After that, it would be advisable to perform resistance tests for several different models whose geometry is systematically changed to represent the limits of practical Tri-SWACH designs. Using the experimental data collected the ANN could be retrained and validated as a resistance prediction tool, drawing on the ANN's ability to interpolate results.

 

Additionally, a comparison of Tri-SWACH resistance to other hull forms would be of interest. Based on intuition, one would speculate that Tri-SWACH vessels would display resistance characteristics similar to trimaran hull forms but with potential performance benefits overall given that the central hull would generate less wave-making resistance than a traditional trimaran central hull. Less wave generation would also reduce the interference effects traditional experienced by trimaran hull forms. However, further research using similarly proportioned hull forms would need to be undertaken to verify this hypothesis.

## 7. ACKNOWLEDGEMENTS

The authors wish to thank Professor John Shawe-Taylor and Dr Denise Gorse from the UCL Department of Computer Science for time spent imparting some of their knowledge of artificial neural networks, which was invaluable to this work's success.

The authors also wish to thank the ACCeSS programme for permitting the use of their experimental data and research. The ACCeSS Centre is funded by the United States Navy's (USN) Office of Naval Research (ONR) under Grant Award No. N00014-10-1-0652. Without this programme, it would not have been possible to investigate the viability of an ANN for Tri-SWACH resistance prediction for preliminary ship design. Additional support for one author was also received from a UK Royal Academy of Engineering Global Research Award.

## 8. REFERENCES

1. GOUGOULIDIS, G. 'The Utilization of Artificial Neural Networks in Marine Applications: An Overview'. *Naval Engineering Journal, vol. 120, no. 3, pp19-26 American Society of Naval Engineers*. 2008.
2. COUSER, P., MASON, A., MASON, G., SMITH, C., & VON KONSKY, B.. 'Artificial Neural Networks for Hull Resistance Prediction'. *In 'Proc. 3rd International Conference on Computer Applications and Infor- mation Technology in the Marine Industries (COMPIT)', pp. 391-402, Siguenza, Spain.* 2004.
3. ROYCE, R., MOURAVIEFF, A., & ZUZICK, 'A Trimaran Resistance Artificial Neural Network'. *In Proc. 11th International Conference on Fast Sea Transportation* (*FAST 2011), pp717-726, Honolulu, Hawaii, USA.* September, 2011.
4. AUSTAL. 'Wind Express Tri-SWATH 27'. *Retrieved August 3, 2012 from http://www.austal.com/en*. 2012.
5. FJELLSTRAND. 'Breakthrough Order for New Innovative Concept in Offshore Wind Market'. *Retrieved August 16, 2012 from http://www.fjellstrand.no/*. 2012
6. CARR, B., & DVORAK, R. 'Investigation of Trimaran Interference Effects'. *Research Thesis, Webb Institute, Glen Cove, New York, USA*. 2007.
7. KLAG, J., & MCMAHON, I. 'Calm Water Resistance Study of a Novel Trimaran'. *Research Thesis, Webb Institute, Glen Cove, New York, USA*. 2011.
8. ROYCE, R., & MCDONALD, T. 'Tri-SWACH Resistance: Comparison of Experimental and Numerical Results'. *Internal ACCeSS Technical Report, UCL London, UK*. 2012.
9. LAZAUSKAS, L. 'Resistance, wave-making and wave-decay of thin ships, with particular emphasis on the effects of viscosity', PhD Thesis, Applied Mathematics, The University of Adelaide, 20 April 2009
10. KRING, D.C., MILEWSKI, W.M., & FINE, N.E. 'Validation of a NURBS-based BEM for multihull ship seakeeping'. 25th Symposium on Naval Hydrodynamics, St. John's, Newfoundland, Canada. 2004
11. SCHMIDT, A. 'Multilayer Neural Network'. *Retrieved 20 August 2012 from http://www.teco.uni-karlsruhe.de/~albrecht/neuro/html/node18.html.* 2012
12. CHEUNG, V., & CANNONS, K. 'An Introduction to Neural Networks'. *Signal and Data Compression Group, University of Manitoba,* May, 2002.
13. HASSOUN, M. 'Fundamentals of Artificial Neural Networks'. *Massachusetts Institute of Technology Press, London, UK*. 1995.
14. PATTERSON, D. 'Artificial Neural Networks: Theory and Applications'. *Prentice Hall, Simon & Schuster*, *Singapore,* 1996.
15. BEALE, M., HAGAN, M., & DEMUTH, H. 'Neural Network Toolbox User's Guide'. *The MathWorks, Inc*. 2012.
16. "Generalization." *Merriam-Webster Dictionary*. *http://www.merriam-webster.com*. 11 December 2011.
17. 'ITTC Recommended Procedures'. *International Towing Tank Committee. Publisher SNAME, Jersey City, NJ. SNAME, Jersey City, NJ.* November, 2011.
18. DUBROVSKY, V., & LYALHOVITSKY, A. 'Multi-hull Ships'. *SNAME, Jersey City, NJ*. 2001.

**ANNEX A - Statistical Methods Applied to ANN Performance Prediction**

The performance of each ANN can be quantified by a variety of statistical methods:

i. Root Mean Square (RMS):

$$RMS = \sqrt{\frac{1}{n}\sum_{i=1}^{n}[f_i - y_i]^2} \qquad \text{Eq. 2}$$

ii. Mean Squared Error (MSE):

$$MSE = \frac{1}{n}\sum_{i=1}^{n}[f_i - y_i]^2 \qquad \text{Eq. 3}$$

iii. Mean Absolute Error (MAE):

$$MAE = \frac{1}{n}\sum_{i=1}^{n}|f_i - y_i| \qquad \text{Eq. 4}$$

iv. Mean Absolute Percentage Error (MAPE):

$$MAPE = \frac{100\%}{n}\sum_{i=1}^{n}\left|\frac{f_i - y_i}{y_i}\right| \qquad \text{Eq. 5}$$

Where

| | |
|---|---|
| $f_i$ | Is the actual experimental value (actual target) |
| $y_i$ | Is the ANN generated output (predicted value) |
| n | Is the number of values |